# Deep Fusion Feature Representation Learning With Hard Mining Center-Triplet Loss for Person Re-Identification

Cairong Zhao, Xinbi Lv, Zhang Zhang, Wangmeng Zuo, *Senior Member, IEEE*, Jun Wu, *Senior Member, IEEE*, and Duoqian Miao

***Abstract*—Person re-identification (Re-ID) is a challenging task in the field of computer vision and focuses on matching people across images from different cameras. The extraction of robust feature representations from pedestrian images through CNNs with a single deterministic pooling operation is problematic as the features in real pedestrian images are complex and diverse. To address this problem, we propose a novel center-triplet (CT) model that combines the learning of robust feature representation and the optimization of metric loss function. Firstly, we design a fusion feature learning network (FFLN) with a novel fusion strategy consisting of max pooling and average pooling. Instead of adopting a single deterministic pooling operation, the FFLN combines two pooling operations that can learn high response values, bright features, and low response values, discriminative features simultaneously. Our model obtains more discriminative fusion features by adaptively learning the weights of the features learned by the corresponding pooling operations. In addition, we design a hard mining center-triplet loss (HCTL), a novel improved triplet loss, which effectively optimizes the intra/inter-class distance and reduces the cost of computing and mining hard training samples simultaneously, thereby enhancing the learning of robust feature representation. Finally, we proved our method can learn robust and discriminative feature representations for complex pedestrian images in real scenes. The experimental results also illustrate that our method achieves an 81.8% mAP and a 93.8% rank-1 accuracy on Market1501, a 68.2% mAP and an 83.3% rank-1 accuracy on DukeMTMC-ReID, and a 43.6% mAP and a 74.3% rank-1 accuracy on MSMT17, outperforming most state-of-the-art methods and achieving better performance for person re-identification.**

***Index Terms*—Person re-identification, center-triplet model, fusion feature representation, hard mining center-triplet loss.**

Manuscript received May 31, 2019; revised October 22, 2019 and December 27, 2019; accepted January 30, 2020. Date of publication February 6, 2020; date of current version November 18, 2020. This work was supported in part by the National Natural Science Foundation of China under Grants 61673299, 61203247, 61573259, and 61573255 and in part by the Fundamental Research Funds for the Central Universities and the Open Project Program of the National Laboratory of Pattern Recognition. The authors contribute equally to this work. The associate editor coordinating the review of this manuscript and approving it for publication was Dr. Ramazan S. Aygun. *(The authors contributed equally to this work.) (Corresponding author: Cairong Zhao.)*

Cairong Zhao, Xinbi Lv, Jun Wu, and Duoqian Miao are with the Department of Computer Science and Technology, Tongji University, Shanghai 1238, China (e-mail: zhaocairong@tongji.edu.cn; 1833028@tongji.edu.cn; wujun@tongji.edu.cn; dqmiao@tongji.edu.cn).

Zhang Zhang is with the CRIPAC and NLPR, Institute of Automation, Chinese Academy of Sciences, Beijing 100190, China, and also with the UCAS, Beijing 100049, China (e-mail: zzhang @nlpr.ia.ac.cn).

Wangmeng Zuo is with the School of Computer Science and Technology, Harbin Institute of Technology, Harbin 150090, China (e-mail: cswmzuo@gmail.com).

Color versions of one or more of the figures in this article are available online at https://ieeexplore.ieee.org.

Digital Object Identifier 10.1109/TMM.2020.2972125

## I. Introduction

PERSON Re-Identification (Re-ID) aims to match two pedestrian images from non-overlapping camera views. Due to the large visual variations in illumination, posture, viewpoint, misalignment, and background occlusions, person re-identification is a difficult task; some challenging examples are shown in Fig. 1.

With the development of deep convolution neural networks (CNNs), an increasing number of works on Re-ID are seeking to design and train an end-to-end model directly to learn robust feature representation from pedestrian images. There are two key areas that comprise CNN-based work, the design of convolution neural networks and the design of the metric loss function.

In the process of designing a CNN, most previous methods use self-designed CNN architectures to learn feature representation, such as the filter pairing neural network (FPNN) [1], the fusion feature net (FFN) [2], PersonNet [3], Spindle Net [4], the multi-scale context-aware network (MS-CAN) [5], the pedestrian alignment network (PAN) [6], etc. It is generally accepted that deeper networks can enrich the granularity of features and bring significant performance improvements. Thus, an increasing number of methods apply the classic pretrained model (VGGNet [7], GoogLeNet [8], ResNet [9]) to learn more discriminative deep features considering their deeper network structures and competitive performance, such as TriNet [10], AlignedReID [11], attribute-person recognition network (APN) [12], pose-sensitive embedding (PSE) [13], the harmonious attention network (HA-CNN) [14], and the global-local-alignment descriptor (GLAD) [15]. The pretrained models extract deep features of images with deeper convolution layers. To avoid generating deep features with a higher dimensionality, the pooling layer is usually needed to reduce the resolution of the features and transform the deep feature representation into a more usable one that preserves discriminative information while discarding redundant details [16], [17], so as to overcome variations in illumination, posture, viewpoint, misalignment, and background occlusion. Average pooling and max pooling are two popular


Fig. 1. Some image pairs from the Market1501 [36] dataset. The upper and lower adjacent images have the same identity: (a) variations in illumination, (b) variations in posture, (c) variations in viewpoint, (d) variations in misalignment, and (e) variations in background occlusion.

methods adopted for computational efficiency. For example, the original ResNet50 adopts a global average pooling to transform a deeper feature representation into a simple 2048-d feature vector. However, it has some limitations in extracting a more robust feature representation. As Yu *et al*. argued in [17], both the average pooling and max pooling operators have their own drawbacks. Sometimes, they will produce unacceptable results. For example, average pooling calculates the mean of all the pixels within the pooling region, which will take all the low response values into consideration. As illustrated in Fig. 2(a), if there are many zero values, the contrast in the feature map will be reduced significantly. Regarding max pooling, it only considers the maximum response values and ignores the others in the pooling region. If most of the responses in the pooling region have high values, the distinguishing features will vanish after max pooling, as shown in Fig. 2(b).

Learning robust and discriminative feature representation through a single deterministic pooling operation remains challenging because the features in pedestrian images from real scenes are more complex and diverse. To solve this problem, we propose a fusion feature learning network (FFLN). The FFLN combines max pooling and average pooling instead of adopting a single deterministic pooling operation, which learns high response values, bright features, and low response values, discriminative features simultaneously. It also obtains more discriminative fusion features by adaptively adjusting the weights of features learned by corresponding pooling operations.

During the process of designing a metric loss function, most previous works regard person re-identification as a multiple classification task that usually adopts a softmax loss to train and optimize their networks for learning discriminative feature representation. However, these methods still incur a high error rate when classifying samples. The studies [19]–[21], [10], [22]–[25] focus on minimizing the intra-class distance and maximizing the inter-class distance to learn more discriminative features. Typical methods are triplet loss [19] and center loss [20].

However, center loss and triplet loss still have some shortcomings. Center loss is only designed to pull samples of the same class to the center without maximizing the inter-class distance. Triplet loss optimizes the distribution of triplets by requiring the distance from the anchor to the positive (intra-class) samples to be less than the distance of the anchor from the negative (inter-class) samples to be meet a predefined margin, without considering minimizing the intra-class distance, which usually produces a relatively large cluster of intra-class samples. In addition, it results in a massive dataset of triplets, including many negative triplets, that requires training. Furthermore, the negative triplets meeting the constraint condition of triplet loss will not contribute to the training of the model, as shown in Fig. 3. To deal with the problem of triplet loss, some improved methods have been proposed, such as improved triplet loss [21], trihard loss [10], quadruplet loss [22], margin sample mining loss [23], point-to-set (HAP2S) loss [24], etc. They are better at minimizing the intra-class distance and maximizing the inter-class distance at the same time. Although the performance of Re-ID has been improved, it still requires the mining and training of hard triplets, which is a huge time consuming process. Thus, the aim of designing a metric loss function is not only to minimize the intra-class distance and maximize the inter-class distance but also to reduce the cost of computing and mining hard training samples as much as possible.

Recently, two novel methods have provided a new approach, namely class-wise triplet loss (CWTL) [26] and triplet-center loss (TCL) [27]. They both successfully combine the ideas of triplet loss and center loss to address the above-mentioned problems. Inspired by them, we propose a loss known as hard mining center-triplet loss (HCTL), also with the aim of realizing the optimization of the intra/inter-class distance and reducing the cost of computing and mining hard training samples simultaneously.

We propose an overall framework named the center-triplet (CT) model in this paper, which combines the learning of robust feature representation and the optimization of metric loss function. Specifically, we firstly extract deep fusion features from input images through the fusion feature learning network (FFLN). Then, we adopt hard mining center-triplet loss to train the model for optimizing the intra/inter-class distance and reducing the cost of computing and mining hard training samples simultaneously, thereby achieving more discriminative feature representation.

Finally, we describe the motivation and contribution of this paper as follows.

*Motivation:* There are some limitations in the many existing methods:

1) Many approaches have difficulties in learning more discriminative feature representations through a single deterministic pooling operation.
2) Many metric learning losses have difficulties in realizing the optimization of the intra/inter-class distance and reducing the cost of computing and mining hard training samples simultaneously.

*Contribution:* The main original contributions of our work are summarized as follows:

1) We present a novel center-triplet model, combining the learning of robust feature representation and the optimization of metric loss function, which outperforms most state-of-the-art methods and achieves superior performance in person re-identification.
2) We propose a fusion feature learning network (FFLN), to combine max pooling and average pooling, which learns

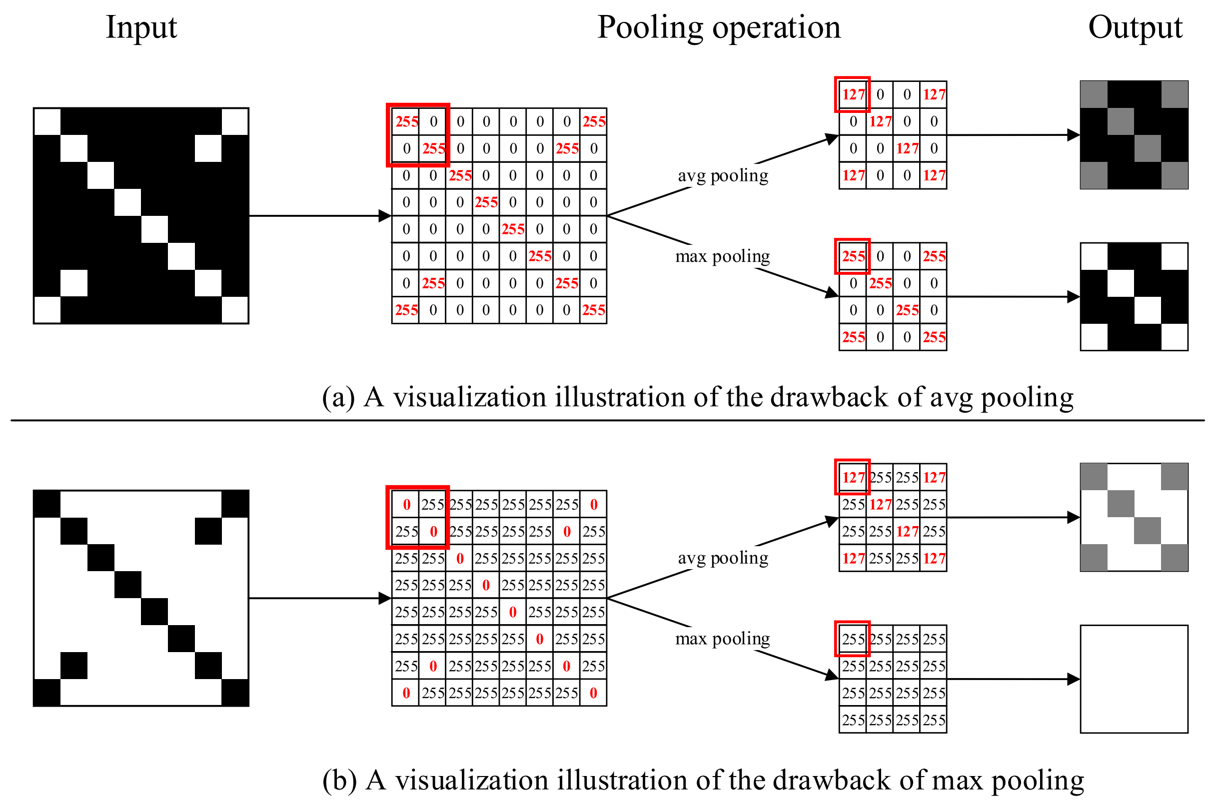


Fig. 2. Simple samples illustrate the drawbacks of max pooling and avg pooling. Input denotes the input image sample, Output denotes the learned feature, and the numbers in the box represent the response values. (a) An illustration of the drawbacks of avg pooling, where the features learned by avg pooling do not represent the input image as well as the features learned from max pooling. (b) An illustration of the drawbacks of max pooling, where the features learned by max pooling do not represent the input image as well as the features learned by avg pooling.

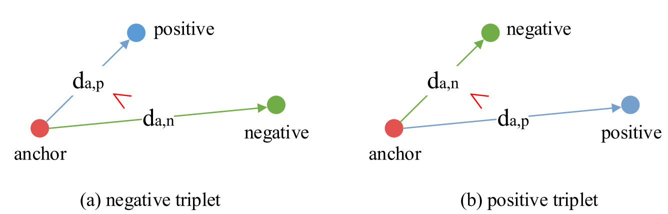


Fig. 3. Two kinds of triplets. (a) Negative triplet with *da, p* $<$ *da, n*, *da, p* denotes the relative distance of the anchor to the positive sample, *da, n* denotes the relative distance of anchor to the negative sample. (b) Positive triplet with *da, n* $<$ *da, p*.

high response values, bright features, and low response values, discriminative features simultaneously. It also obtains more discriminative feature representation by adaptively learning the weights of the features corresponding to different pooling operations.

3) We propose a hard mining center-triplet loss, a novel improved triplet loss, which effectively realizes the optimization of the intra/inter-class distance and reduces the cost of computing and mining hard training samples simultaneously, thereby enhancing the learning of robust feature representation.

The paper is organized as follows: In Section II, we review some related works about person re-identification. Section III elaborates on the proposed center-triplet model. Section IV presents the experimental results of the comparisons and evaluation. Finally, the conclusion is drawn in Section V.

## II. Related Work

Most of the existing deep learning methods for person re-identification generally fall into two categories. The first group of methods focus on designing simple and efficient convolutional neural networks to extract discriminative features that are robust to variations in illumination, posture, viewpoint, misalignment, and background occlusions, etc. The second group of methods mainly focus on designing robust distance metrics loss functions to deal with complex matching problems, thereby optimizing the network to more effectively learn feature representation.

### A. *Convolutional Neural Network*

Traditional approaches have focused on low-level features, such as color features [28] and texture features [29]. However, low-level features are not sufficiently robust to large variations in appearance. To address it, Zhao *et al*. proposed a novel method named Multiple Metric Learning based on the Bar-shape Descriptor (MMLBD) [30] to capture the intrinsic structure information hidden in different person images. This was achieved through the multiple bar-shape descriptor that makes full use of spatial correlation between center points and their neighbors, which better represents the appearance of a person with the changes of illumination, rotation, translation and perspective for Re-ID. In [31], a descriptor called Maximal Granularity Structure Descriptor (MGSD) was proposed. This can capture rich local structural information from overlapping macro-pixels in an image, and analyze the horizontal occurrence of multi-granularity and maximize their occurrence in order to extract a robust representation for viewpoint changes. In [32], the similarity learning with joint transfer constraints model was proposed to alleviate the inconsistency of data distributions in terms of viewpoint changes and illumination variations. With the development of deep learning, researchers began to explore how to make a model to learn robust deep features automatically instead of the traditional hand-designed features. For example, in [1], Li *et al.* first proposed a deep filter pairing neural network (FPNN) that jointly optimizes feature learning, photometric transforms, geometric transforms, misalignment, occlusions, and classification within a unified deep architecture. It was the first work to employ deep learning to person re-identification problems. In [2], the feature fusion net (FFN) was proposed to learn robust fusion features by jointly utilizing CNN features and hand-crafted features. In [54], the multilevel triplet deep learning model (MT-net) was proposed to combine fine, shallow layer information with coarse, deeper layer information to learn a better feature representation. Zhao *et al.* proposed SpindleNet [4], which firstly extracted features from several body regions and then merged them to learn more discriminative fusion features. In [15], Wei *et al.* proposed the GLAD framework, which explicitly leverages the local and global cues in the human body to generate a discriminative and robust representation. There are also some methods [5], [11] learning powerful features by jointing global features with local body-part features.

However, it remains very challenging to learn robust features which are discriminative, reliable, and invariant to the large variations in illumination, posture, viewpoint, misalignment, and background occlusion, etc. In order to solve this problem, we propose a fusion feature learning network (FFLN) for learning discriminative feature representation.

### B. Metric Loss Function

Traditional deep metric learning methods regard person re-identification as a multiple classification task and adopt softmax loss to train and optimize their networks. However, these methods usually produce large clusters in intra-class and heavy overlaps in inter-class, thereby having a high error rate. As illustrated in Fig. 4(a), 1, 2, and 3 represent the overlapping areas of different classes.

To better address complex matching problems in image pairs, many improved deep metric learning models have been proposed. Wen *et al.* [20] firstly presented the center loss, by learning a center for the same class samples to pull them to their centers, which has been successfully used for face recognition. In [18], Ding *et al.* proposed a feature affinity-based pseudo labeling (FAPL) approach, which also adopted softmax loss joint with center loss to train the network to ensure discriminative feature representation learning. Specifically, the center loss can

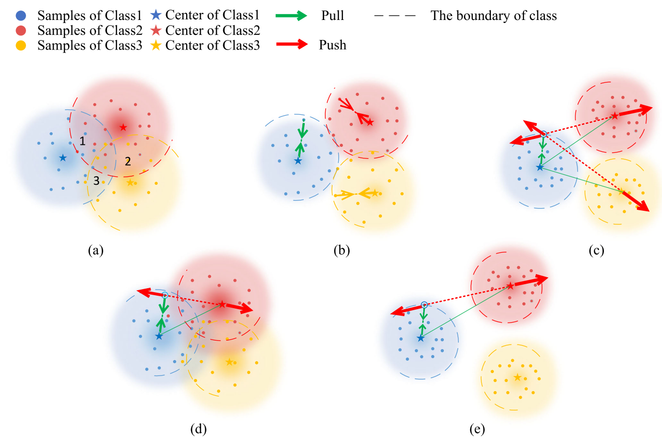


Fig. 4. An illustration of the distributions of deeply-learned features by (a) softmax loss, (b) softmax loss + center loss, (c) softmax loss + class-wise triplet loss, and (e) softmax loss + triplet-center loss. (d) Describes the idea of the triplet-center loss with hard sample mining. Randomly selected identities from the testing set of Market1501 [36]. The points with different colors denote features from different identities. The pentagrams denote the centers of classes.

be formulated as:

$$L_c = \frac{1}{2}\sum_{i=1}^{P\times K}\left\|f_i - c_{y^i}\right\|_2^2, \tag{1}$$

where $P$ denotes the number of classes in a mini-batch, $K$ denotes the number of samples in each class, the $c_{y^i}$ denotes the deep features of $y^i$th class center, which is computed by averaging the features of the corresponding classes of the mini-batch, and $f_i$ denotes the deep features of $i$th sample.

Since the centers are used within each mini-batch instead of the whole training set, their updates are very unstable. It must be completed under the joint supervision of softmax loss during the training process, which provides good guidance in seeking better class centers. However, center loss does not consider how to enlarge the inter-class distance, and it still contains a few overlaps in the inter-class, as shown in Fig. 4(b).

The successful application of facenet in face recognition has led researchers to focus on how to efficiently select triplets to train the end-to-end network for Re-ID. Ding *et al.* [19] made the first attempt to use a triplet framework to extract the features of samples and then calculate triplet loss to optimize the network learning process. Triplet loss aims at ensuring the intra-class distance is less than the inter-class distance by a predefined margin $m$, which can be computed as:

$$L_{tri} = \sum_{\substack{a,p,n \\ y_a = y_p \neq y_n}} \max\left(d_{a,p} - d_{a,n} + m, 0\right), \tag{2}$$

where $a$, $p$, $n$ denote the anchor, positive sample, and negative sample in each triplet, respectively, $d_{a,p}$ denotes the relative distance of the positive sample to the anchor, $d_{a,n}$ denotes the relative distance of the negative sample to the anchor, and $m$ is the margin that is enforced between positive and negative pairs.

The classic triplet loss has two problems. One is the clustering effect of the model is not significant because the loss does not consider how to minimize the intra-class distance. Another is that a sharply increasing number of triplets including many negative triplets with the explosive increasing of dataset, and the use of a large and unbalanced number of negative triplets could also produce poor results. Some improved methods are proposed based on triplet loss to solve the above problems.

To deal with the problems of triplet loss, some improved methods have been proposed. Cheng *et al.* [21] optimized the training process of the triplet framework by adopting an improved triplet loss function, which requires reducing the distance between pairs from the same class to less than a margin $\alpha$ ($\alpha$ is much less than $m$). Hermans *et al.* [10] proposed the trihard loss (triplet loss with hard sample mining), which aims at selecting the hardest triplets for training. Yu *et al.* [24] proposed the hard-aware point-to-set (HAP2S) loss with an adaptive hard mining scheme, which aims at assigning higher weights to the hard samples to compute triplet loss. But the cost of computing and mining the hard triplets is enormous. In addition, Ali *et al.* [25] proposed a nullspace kernel maximum margin metric learning (NK3ML) framework, which efficiently minimizes the intra-class distance and maximizes the inter-class distance. We do not discuss it here because it addressed the small sample size (SSS) problem.

In summary, it is not optimal to only consider the optimization of the intra/inter-class distance. Optimization to reduce the cost of computing and mining hard samples is also important when training the model. Recently, two novel studies have attracted attention.

Ming *et al.* [26] proposed the class-wise triplet loss (CWTL) for face recognition. Different from classic triplet loss, it aims to decrease the distance between the anchors and the intra-class centers and enlarge the distance of the anchors from the inter-class centers by learning the centers of the classes of samples and using them instead of individual samples as the positives and negatives to form the triplets, which can significantly reduce the number of triplets involved in training the model, thereby reducing the cost of calculation loss. The CWTL can be formulated as follows:

$$L_{cwt} = \sum_{i=1}^{P\times K} \sum_{l=1, l\neq y^i}^{P} \max\left(D\left(f_i, c_{y^i}\right) - D\left(f_i, c_l\right) + m, 0\right), \tag{3}$$

where $D(f_i, c_{y^i})$ represents the squared Euclidean distance function denoted as follows:

$$D\left(f_i, c_{y^i}\right) = \left\| f_i - c_{y^i} \right\|_2^2, \tag{4}$$

As illustrated in Fig. 4(c), the CWTL effectively solves the problems of large clusters within the intra-class and overlaps within the inter-class.

Another is the work by He *et al.* [27], which proposed a novel loss function named triplet-center loss (TCL) for Multi-View 3D Object Retrieval. They argued that center loss still results in small overlaps within the inter-class samples because it only aims at minimizing the intra-class distance, as illustrated in Fig. 4(b). Specifically, the proposed TCL can ensure the distance between the samples and their corresponding center $c_{y^i}$ is less than the distance between the samples and their nearest negative center $c_l$ by a margin *m*. The TCL could be computed as follows:

$$L_{tc} = \sum_{i=1}^{P\times K} \max\left(D\left(f_i, c_{y^i}\right) - \min_{l\neq y^i} D\left(f_i, c_l\right) + m, 0\right), \tag{5}$$

An illustration of the distributions of samples learned by TCL can be seen in Fig. 4(d)–(e).

Inspired by CWTL and TCL, we design a hard mining center-triplet loss, a novel improved strategy of triplet loss that mines novel hard triplets for training. Finally, our loss effectively optimizes the intra/inter-class distance and reduces the cost of computing and mining hard training samples simultaneously.

In general, we put forward a novel center-triplet (CT) model for person re-identification, which combines the learning of robust feature representation and the optimization of metric loss function. In the next section, we will present our method in detail.

## III. Proposed Center-Triplet Model

Our center-triplet model is designed based on the classic triplet framework. The overall framework of our model is shown in Fig. 5. It is composed of two parts, the learning of fusion feature representation and the optimization of metric loss function. We first describe the overall framework of our method in Section III-A. Then, we elaborate on the design of the fusion feature learning network (FFLN) in Section III-B and the design of our metric loss function in Section III-C. In Section III-D, we compare the proposed model with similar methods for Re-ID. Finally, the processes of training and optimizing our model are introduced in Section III-E.

### A. The Overall Framework

As illustrated in Fig. 5, our model uses mini-batch images to train the network. In each mini-batch, images are resized into 256 $\times$ 128 pixels as inputs, and the 2048-d deep fusion features are extracted through the FFLN. Then, the model will learn the centers of classes of these fusion features and mine novel hard triplets to calculate loss by the proposed hard mining center-triplet loss (HCTL). The HCTL is better at minimizing intra-class distance and maximizing inter-class distance, thereby optimizing the network to learn more robust feature representation. Finally, the model provides a significant performance improvement for Re-ID.

### B. The Fusion Feature Learning Network (FFLN)

The proposed fusion feature learning network is modified based on the original ResNet50. As shown in Fig. 6, the FFLN mainly consists of the following distinct layers: convolution layer, mixed pooling layer, and fusion layer. Next, we introduce each of these layers in detail.

*Convolution layer:* We employ the convolution layers of ResNet50 as basic convolution layers. However, considering that higher spatial resolution may enrich the granularity of features and result in significant performance improvements, we try to set the last stride (last spatial down-sample operation) in the

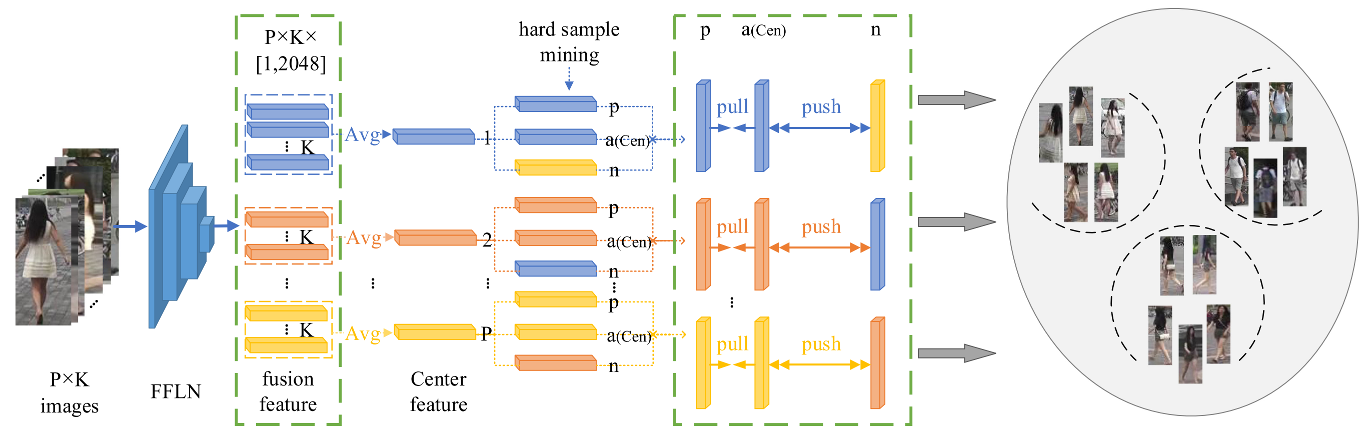


Fig. 5. The overall framework of the proposed Center-Triplet model, where $P$ denotes the number of classes in a mini-batch, $K$ denotes the number of samples in each class, *a(cen)* denotes the center feature of each class samples, *p* denotes the hardest positive sample that is farthest to the *a(cen)* with the same class label, and *n* denotes the hardest negative sample that is closest to the *a(cen)* with the different class label, Avg denotes getting the center feature by the averaging operation. Specifically, $P \times K$ images are fed to the FFLN to get the 2048-d deep fusion features. Then, the HCTL will learn the center features of classes of these fusion features and mine the hardest triplets to train and optimize the model for learning discriminative features, which could pull the intra-class samples closer and push the inter-class samples further away.

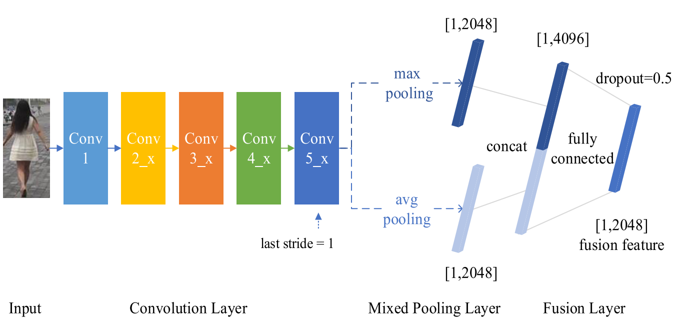


Fig. 6. Proposed Fusion Feature Learning Network (FFLN).

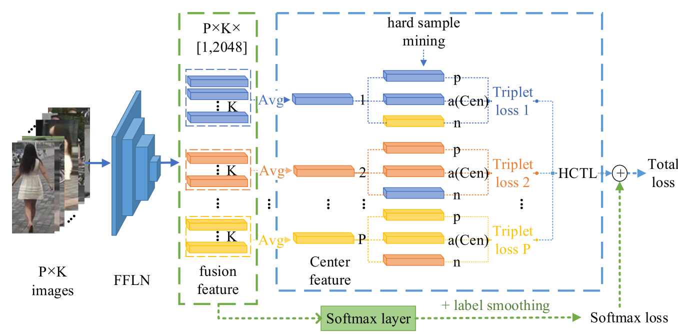


Fig. 7. Proposed metric loss function, hard mining center-triplet loss (HCTL). The HCTL joints with softmax loss to optimize the overall model.

Conv5 layer from 2 (the last stride of the original ResNet50) to 1 to obtain a larger feature map ($16 \times 8$) than the original size ($8 \times 4$).

*Mixed pooling layer:* Convolution layers followed by the mixed pooling layer consist of two parts, the max pooling layer and the average pooling layer. We deal with the output of the Conv5 layer with max pooling and average pooling at the same time instead of using a single deterministic pooling operation. Then, these two sub-part features are linked together to form a high dimensional feature vector of 4096-d for learning deep fusion features in the following fusion layer.

*Fusion layer:* In the fusion layer, we mainly append a fully-connected layer followed by Batch Normalization (BN) and a Rectified Linear Unit (ReLU). The fully-connected layer obtains more discriminative fusion features by adaptively learning the weights of features, which are learned by pooling operations. In addition, we apply dropout [33] on the fully-connected layer to effectively avoid overfitting and gain considerable performance improvements. Finally, the network will output a 2048-d fusion feature for training.

Instead of selecting a single deterministic pooling operation, the FFLN combines max pooling and average pooling. It, therefore, learns appropriate weight parameters for the corresponding pooled features through the fusion layer (fully-connected layer), which can learn high response values, bright features, and low response values, discriminative features simultaneously. It also obtains more robust features to ultimately represent complex pedestrian images in real scenes. In Section IV-D, we elaborate on the advantages of FFLN in feature representation.

### C. Hard Mining Center-Triplet Loss Function (HCTL)

Inspired by CWTL and TCL, we propose a metric loss function named hard mining center-triplet loss (HCTL), a novel improved strategy of triplet loss. As shown in Fig. 7, it aims to learn the centers of the classes of samples and use them instead of individual samples as the anchors to form the hard triplets. Specifically, we firstly regard the centers of all classes in the mini-batch as the anchors. For each center, we select the hardest positive sample which has the farthest distance to it with the same class label and the hardest negative sample which has the closest distance to it with a different class label. Then, we use them to form the hard triplet for computing the triplet loss. The HCTL will control the distance between the center $c_p$ and its farthest positive sample less than the distance between

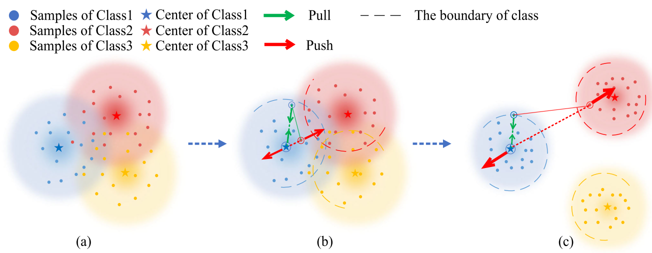


Fig. 8. An illustration of the distributions of deeply-learned features learned by (a) softmax loss and (c) softmax loss + HCTL. (b) Describes the process of mining the hardest triplets. The points with different colors denote deep features from different identities in the Market1501.

the center $c_p$ and its nearest negative sample by a predefined margin $m$.

In summary, the hard mining center-triplet loss is defined as follows:

$$L_{hct} = \frac{1}{P}\sum_{p=1}^{P} \max\left(\max_{1\leq i\leq K}\left(D\left(c_p, f\left(p^i\right)\right)\right) - \min_{\substack{l\neq p, 1\leq l\leq P,\\ 1\leq j\leq K}}\left(D\left(c_p, f\left(l^j\right)\right)\right) + m, 0\right), \tag{6}$$

where $c_p$ denotes the deep features of $p$th class center and $f(p^i)$ denotes the deep features of the $i$th sample in $p$th class.

As the update of centers of the classes could be unstable in a mini-batch with the HCTL, we combine it with softmax loss for training. To improve the guidance provided by softmax in seeking better class centers, we use label-smoothing regularization (LSR) [34] to optimize the calculation of softmax loss. Thus, HCTL and softmax loss is divided into two parts and calculated separately. For the former, the features of centers of classes of training samples are learned by averaging the features of the corresponding classes, and then the hard triplets will be mined to compute HCTL by using a hard sample mining strategy. For the latter, the deep fusion features, the output of FFLN will be calculated using the softmax loss through an added softmax layer. Finally, we need a hyper-parameter $\lambda$ to balance our loss and softmax loss to calculate the total loss, which can be formulated as follows:

$$L = L_{cls} + \lambda L_{hct}, \tag{7}$$

where $L_{cls}$ denotes the softmax loss, $L_{hct}$ denotes the HCTL, and $\lambda$ is the weight used to balance the HCTL and softmax loss.

An illustration of the distributions of samples learned by HCTL joined with softmax loss can be seen in Fig. 8.

### D. Model Analysis and Comparison

In this section, we compare the proposed model with similar methods used in feature representation and the optimization of metric loss function.

*Comparison in terms of feature representation:* Because the proposed fusion feature learning network is modified based on the original ResNet50 and aims at addressing the drawbacks of adopting a single deterministic pooling operation, we mainly compare it with the ResNet50 (with a single deterministic pooling operation) in regards to feature representation. The ResNet50 usually extracts the deep features of inputs with standard convolution layers, followed by a global average pooling operation. In contrast, we have the following differences:

1) Firstly, we try to set the last stride in the Conv5 layer from 2 to 1 to get a feature map with a higher spatial resolution for enriching the granularity of features. It was inspired by the following paper. In [35], Luo *et al.* proved that the ResNet50 with the last stride modified to 1 shows obvious improvements over the original ResNet50 with the last stride set to 2.
2) In addition, both the average pooling and max pooling operations have their drawbacks. It is hard to attain discriminative feature representation for complex images by adopting a single deterministic pooling operation. Thus, we propose a fusion strategy consisting of two pooling operations. We modify the original pooling layer by adding an extra max pooling and adding the fusion layer to learn the weights of the corresponding features adaptively, which aims at learning high response values, bright features, and low response values, discriminative features simultaneously and obtains more robust fusion features.

*Comparison of the optimization of the metric loss function:* Now most common models adopt softmax loss, center loss, triplet loss, or variations of these (improved triplet loss, trihard loss, HAP2S loss, etc.), or a combination of these (class-wise triplet loss, triplet-center loss) to optimize networks. Obviously, triplet loss and its varieties including class-wise triplet loss and triplet-center loss have a common idea: a hard sample mining strategy. All of them randomly select one sample as an anchor to build a triplet that will produce many triplets because each sample in the mini-batch has to be selected at least once. The hard sample mining strategy of HCTL contains a fundamental difference. It makes the first attempt that uses the center of class, instead of the individual sample, as the anchor, the farthest positive sample as the positive, and the nearest negative sample as the negative to form the novel hard triplet for calculating triplet loss. Based on such a modification, the number of triplets produced can be reduced significantly.

Specially, we randomly select $P$ classes of samples and then randomly sample $K$ images from each class to form a mini-batch for training. This will result in a large number of $P \times K \times (K\text{-}1) \times (P\text{-}1) \times K$ triplets. Since CWTL uses the centers of the classes to represent the global distribution of the classes rather than the individual samples, which only have $K$-1 triplets for each sample, in total there is a set of $P \times K \times (K\text{-}1)$ triplets to be chosen to train CNN by using CWTL. The design of TCL combines the advantages of trihard loss and center loss. For each sample, TCL only selects the hardest negative center as a negative to form the triplet, which produces one triplet for each anchor. Finally, $P \times K$ triplets will be constructed for one mini-batch, which is the same as trihard loss. Far less than either of them, the HCTL uses the center of class as the anchor, only considers the distance of the center to the farthest intra-class sample and the distance to the closest inter-class sample, and only $P$ hard triplets are selected in each mini-batch, where $P$ is the number of the classes in mini-batch. Thus, the proposed method is more efficient at optimizing the intra/inter-class distance and reducing the cost of computing and mining hard training samples.

In the experiments in Section IV, we compare the proposed method with several similar methods and demonstrate the performance improvements of our method.

### E. Training and Optimization

The proposed model is trained and optimized by HCTL combined with softmax loss. Since the calculation of softmax loss requires an extra softmax layer, we should optimize HCTL and softmax loss separately during back propagation. Let $\{\omega\}$ denote the initialized networks parameters and $f_\omega(i)$ denote the fusion features of the network output of image *i*. The hard mining center-triplet loss in (6) can be expanded as follows:

$$L_{hct} = \frac{1}{P}\sum_{p=1}^{P}\max \left(\max_{1\le i\le K}\left(D\left(\frac{1}{K}\sum_{i=1}^{K} f_\omega\left(p^i\right), f_\omega\left(p^i\right)\right)\right) - \min_{\substack{l\neq p,1\le l\le P,\\ 1\le j\le K}}\left(D\left(\frac{1}{K}\sum_{i=1}^{K} f_\omega\left(p^i\right),\ f_\omega\left(l^j\right)\right)\right) + m, 0\right), \tag{8}$$

To simplify the calculations, let us simplify (8) as follows:

$$D_p = \max_{1\le i\le K}\left(D\left(\frac{1}{K}\sum_{i=1}^{K} f_\omega\left(p^i\right),\ f_\omega\left(p^i\right)\right)\right), \tag{9}$$

$$D_n = \min_{\substack{l\neq p,1\le l\le P,\\ 1\le j\le K}}\left(D\left(\frac{1}{K}\sum_{i=1}^{K} f_\omega\left(p^i\right), f_\omega\left(l^j\right)\right)\right), \tag{10}$$

$$L_{hct} = \frac{1}{P}\sum_{p=1}^{P}\max\left(D_p - D_n + m, 0\right), \tag{11}$$

According to the chain rule, the derivatives of the hard mining center-triplet loss can be computed as follows:

$$\frac{\partial L_{hct}}{\partial \omega} = \begin{cases} \dfrac{\partial D_p}{\partial \omega} - \dfrac{\partial D_n}{\partial \omega} & D_p - D_n + m > 0 \\ 0 & D_p - D_n + m \le 0 \end{cases}, \tag{12}$$

$$\frac{\partial D_p}{\partial \omega} = \max_{1\le i\le K}\left(2\left(\frac{1}{K}\sum_{i=1}^{K} f_\omega\left(p^i\right) - f_\omega\left(p^i\right)\right) \cdot \left(\frac{1}{K}\sum_{i=1}^{K}\frac{\partial f_\omega\left(p^i\right)}{\partial \omega} - \frac{\partial f_\omega\left(p^i\right)}{\partial \omega}\right)\right), \tag{13}$$

$$\frac{\partial D_n}{\partial \omega} = \min_{\substack{l\neq p,1\le l\le P,\\ 1\le j\le K}}\left(2\left(\frac{1}{K}\sum_{i=1}^{K} f_\omega\left(p^i\right) - f_\omega\left(l^j\right)\right) \cdot \left(\frac{1}{K}\sum_{i=1}^{K}\frac{\partial f_\omega\left(p^i\right)}{\partial \omega} - \frac{\partial f_\omega\left(l^j\right)}{\partial \omega}\right)\right), \tag{14}$$

Fig. 9. Example images from Market1501 [36] dataset.

Finally, Algorithm 1 shows the main training procedure followed by our method.

**Algorithm 1:** Hard Mining Center-Triplet Loss Training Algorithm

Input: Training samples $\{I_i\}$. Initialized networks parameters $\{\omega\}$. Initialized softmax layer parameters $\{\vartheta\}$ of softmax loss. Hyperparameter $\lambda$ and learning rate $\mu$. The number of iteration $t \leftarrow 0$.

Output: The networks parameters $\{\omega\}$.

while $t \le T$ do
    $t \leftarrow t + 1$;
    Calculate fusion features of samples $f_{p^k}$ by forward propagation;
    Calculate the distance
    $\max_{1\le i\le K}(D(c_p, f_\omega(p^i)))$, $\min_{\substack{l\neq p,1\le l\le P,\\ 1\le j\le K}}(D(c_p, f_\omega(l^j)))$
    Calculate the total loss $L = L_{cls} + \lambda L_{hct}$
    Calculate the $\frac{\partial L_{cls}}{\partial \omega}$, $\frac{\partial L_{hct}}{\partial \omega}$ by back propagation
    Update the softmax layer parameters $\{\vartheta\}$ of softmax loss $\vartheta^{t+1} = \vartheta^t - \mu^t \cdot \frac{\partial L_{cls}}{\partial \vartheta^t}$
    Update the networks parameters
    $\omega^{t+1} = \omega^t - \mu^t \cdot \frac{\partial L}{\partial \omega^t}$
    $= \omega^t - \mu^t(\frac{\partial L_{cls}}{\partial \omega} + \lambda \cdot \frac{\partial L_{hct}}{\partial \omega})$
end while

## IV. Experiments

In this section, we report on experiments to evaluate our method and compare the obtained results with state-of-the-art methods.

### A. Datasets

We conduct experiments on three representative large-scale datasets, Market1501, DukeMTMC-ReID, and MSMT17, respectively.

Market1501 [36] is one of the largest benchmark datasets for person re-identification, and it contains 32,668 images of 1,501 identities from 6 camera views. Each identity is captured by at most six cameras. There are 751 identities in the training set and 750 identities in the testing set. Fig. 9 shows some example images from this dataset.

Fig. 10. Example images from DukeMTMC-ReID [37] dataset.

Fig. 11. Example images from MSMT17 [52] dataset.

DukeMTMC-ReID [37] is a subset of the DukeMTMC [38] tracking dataset, which contains 36,411 images with 1,812 identities captured from 8 different viewpoints. Specifically, there are 16,522 images with 702 identities for training, 17,661 images with 1,110 identities in the gallery, and another 2,228 images with 702 identities in the gallery for query. Fig. 10 shows some example images from this dataset.

MSMT17 [52] is the current largest public Re-ID dataset, which is collected with different weather conditions during 3 time slots (morning, noon, afternoon). It contains 126,441 images of 4,101 identities captured from 12 outdoor cameras and 3 indoor cameras. The MSMT17 is also significantly more challenging than Market1501 and DukeMTMC-ReID due to more complex scenes. We follow the same training-testing split of [52]. Fig. 11 shows some example images from this dataset.

### B. Implementation Details

We conduct experiments based on Torchreid [53], a mainstream library for deep-learning person re-identification in PyTorch. In the experiments, every 32 images are randomly selected to form a mini-batch for training, which contains 8 identities, and each identity has 4 images. For feature extraction, we set the last stride in the Conv5 layer to 1 to get deep features with a larger spatial area. We also set the dropout ratio to 0.5 to avoid overfitting in the last fully connected layer. For optimization, the standard AMSGrad [39] algorithm is adopted for faster and more robust back propagation and loss convergence. The initial learning rate of softmax loss and the initial learning rate of HCTL are both set to 3e-4.

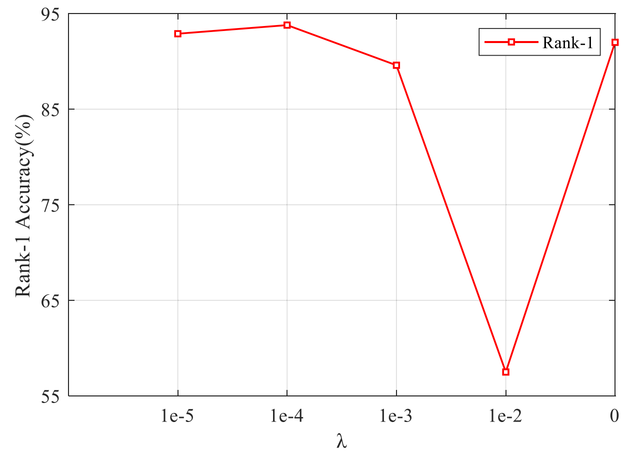


Fig. 12. The influence of weight parameter $\lambda$ evaluated by a score of rank-1 accuracy.

### C. Parameter Influence

In the training process, the model will be trained and optimized by the total loss, as defined by (7). Thus, the margin parameter $m$ and the weight parameter $\lambda$ may affect the final performance of Re-ID. Specifically, $m$ can affect the relative distance between the center to its farthest positive sample and to its nearest negative sample, while $\lambda$ controls the trade-off between HCTL and softmax loss. To study the impact of the two hyper parameters, we conducted experiments on the Market1501 dataset and evaluated the performances with rank-1 accuracies.

To study the impact of weight parameter $\lambda$, we firstly fixed margin $m$ as 0.5, and then set $\lambda$ as 1e-5, 1e-4, 0.001, 0.01, and 0, respectively. The experimental results are presented in Fig. 12. If the model is only trained by softmax loss ($\lambda = 0$), the performance can achieve 92.0% rank-1 accuracy. But with HCTL, we can get the highest improvement of 1.8% in terms of rank-1 when $\lambda$ is set to 1e-4. This is because once the model trained by softmax loss has converged, the appropriate weight of HCTL can further enforce the clustering of features of samples and attain a better performance. For weight $\lambda$, too large or too small values may lead to inferior results. When it is too small, the contribution of HCTL is weakened, while too large values may affect the convergence of softmax loss, thereby producing poorer results.

To study the influence of $m$, we fixed $\lambda$ as 1e-4 and then set $m$ from 0.1 to 1. The experimental results are presented in Fig. 13. For margin $m$, we can also see that too large and too small values both lead to inferior performances. Too small values may weaken the effect of clustering with HCTL, while too large values may cause overfitting of the model. The best performance gains a rank-1 accuracy of 93.8% by setting $m$ to 0.5.

The experimental results demonstrate that our model achieves the best performance on Market1501 when $\lambda$ is 1e-4 and $m$ is 0.5. In addition, we also conduct the same experiments on the DukeMTMC-ReID and MSMT17 datasets to find the optimal parameters. Finally, we set $m$ and $\lambda$ as 0.5 and 1e-4 as the default setting for all the following experimental evaluations on Market1501 and MSMT17, and set $m$ and $\lambda$ as 0.3 and 1e-4 on DukeMTMC-ReID.

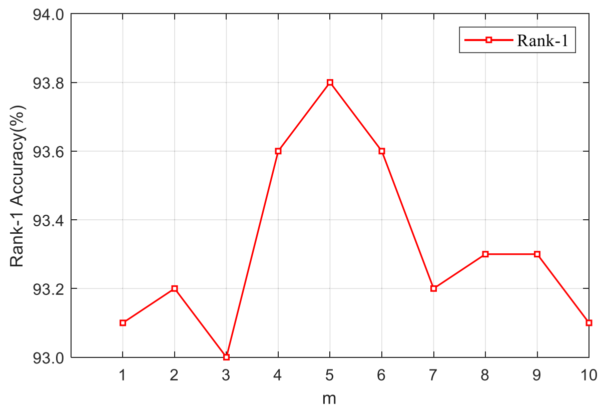


Fig. 13. The influence of margin parameter *m* evaluated by a score of rank-1 accuracy.

TABLE I
COMPARISON WITH STATE-OF-THE-ART METHODS ON MARKET1501 DATASET. 1ST/2ND BEST IN RED/BLUE

| Method | mAP | Rank-1 | Rank-5 | Rank-10 |
|---|---|---|---|---|
| LOMO+XQDA [40] | 22.2 | 43.8 | -- | -- |
| BoW+Kissme [36] | 20.8 | 44.4 | 63.9 | 72.2 |
| Spindle Net [4] | -- | 76.9 | 91.5 | 94.6 |
| SVDNet [41] | 62.1 | 82.3 | -- | -- |
| OIM [44] | 62.5 | 83.0 | 93.1 | 95.2 |
| PAN [6] | 63.4 | 82.8 | 93.5 | -- |
| FAPL[18] | 63.8 | 83.6 | -- | -- |
| GAN [37] | 66.1 | 84.0 | -- | -- |
| APR [12] | 64.7 | 84.3 | 93.2 | 95.2 |
| TriNet [10] | 69.0 | 84.7 | 94.2 | 96.2 |
| MSML [23] | 69.6 | 85.2 | 93.7 | -- |
| HAP2S_E [24] | 69.8 | 84.2 | -- | -- |
| DPFL [46] | 73.1 | 88.9 | -- | -- |
| AlignedReID [11] | 75.9 | 88.8 | 95.6 | 97.4 |
| GLAD [15] | 73.9 | 89.9 | -- | -- |
| MLFN [42] | 74.5 | 90.2 | 95.9 | 97.4 |
| ResNet50-mid [47] | 76.1 | 90.2 | 96.4 | 97.9 |
| Mask Re-ID [48] | 75.4 | 90.4 | -- | -- |
| HA-CNN [14] | 75.6 | 90.9 | 96.4 | 97.8 |
| PCB [43] | 77.3 | 92.3 | 96.9 | 98.2 |
| Deep-Person [49] | 79.6 | 92.3 | -- | -- |
| Ours (last stride=2) | 80.0 | 92.6 | 97.2 | 98.5 |
| **Ours (last stride=1)** | 81.8 | 93.8 | 97.8 | 98.6 |

TABLE II
COMPARISON WITH STATE-OF-THE-ART METHODS ON DukeMTMC-ReID DATASET. 1ST/2ND BEST IN RED/BLUE

| Method | mAP | Rank-1 | Rank-5 | Rank-10 |
|---|---|---|---|---|
| LOMO+XQDA [40] | 17.0 | 30.8 | -- | -- |
| BoW+Kissme [36] | 12.2 | 25.1 | -- | -- |
| GAN [37] | 47.1 | 67.7 | -- | -- |
| APR [12] | 51.9 | 70.7 | -- | -- |
| PAN [6] | 51.5 | 71.6 | 83.9 | -- |
| FAPL[18] | 53.9 | 72.9 | -- | -- |
| OIM [44] | 54.6 | 73.1 | 85.9 | 91.5 |
| TriNet [10] | 57.7 | 74.5 | 86.4 | 89.5 |
| SVDNet [41] | 56.8 | 76.7 | -- | -- |
| HAP2S_E [24] | 59.6 | 76.1 | -- | -- |
| Mask Re-ID [48] | 61.9 | 78.9 | -- | -- |
| DPFL [46] | 60.6 | 79.2 | -- | -- |
| HA-CNN [14] | 63.2 | 80.1 | 89.6 | 92.1 |
| Deep-Person [49] | 64.8 | 80.9 | -- | -- |
| MLFN [42] | 63.2 | 81.1 | 90.3 | 92.6 |
| AlignedReID [11] | 66.7 | 81.6 | 90.4 | 93.1 |
| ResNet50-mid [47] | 64.0 | 81.6 | 90.0 | 93.0 |
| PCB [43] | 66.4 | 81.6 | 91.1 | 93.3 |
| Ours (last stride=2) | 67.9 | 82.9 | 91.3 | 93.6 |
| **Ours (last stride=1)** | 68.2 | 83.3 | 91.7 | 93.8 |

TABLE III
COMPARISON WITH STATE-OF-THE-ART METHODS ON MSMT17 DATASET. 1ST/2ND BEST IN RED/BLUE

| Method | mAP | Rank-1 | Rank-5 | Rank-10 |
|---|---|---|---|---|
| TriNet [10] | 26.9 | 56.9 | 72.7 | 78.4 |
| HA-CNN [14] | 25.5 | 48.8 | 65.7 | 72.2 |
| MLFN [42] | 27.7 | 52.5 | 69.2 | 75.6 |
| GLAD[15] | 34.0 | 61.4 | 76.8 | 81.6 |
| ResNet50-mid [47] | 37.7 | 68.7 | 80.9 | 84.8 |
| PCB [43] | 41.1 | 68.2 | 81.3 | 85.6 |
| Ours (last stride=2) | 40.9 | 71.3 | 82.8 | 86.4 |
| **Ours (last stride=1)** | 43.6 | 74.3 | 84.7 | 87.9 |

### *D. Experimental Results and Analysis*

*1) Comparison With State-of-the-Art Methods:* We conduct experiments with other state-of-the-art methods, including LOMO+XQDA [40], BoW+Kissme [36], Spindle Net [4], SVDNet [41], TriNet [10], AlignedReID [11], HAP2S_E [24], MLFN [42], HA-CNN [14], PCB [43], etc. Then, we evaluate them with rank-1, 5, 10 accuracies and mAP to illustrate the superiority of our proposed model. The results on three datasets are shown in Tables I, II, III and Figs. 14–16.

*Results analysis on Market1501 dataset:* To evaluate the performance of our proposed model, we firstly compare our method with existing state-of-the-art methods on Market1501. As shown in Table I, our method (with the last stride set to 1) is superior to all state of-the-art methods and has the highest scores on rank-1 and mAP. Specifically, it achieves a 93.8% rank-1 accuracy and an 81.8% mAP, which outperforms the Deep-Person by 1.5% (93.8-92.3) in rank-1 and 2.2% (81.8-79.6) in mAP.

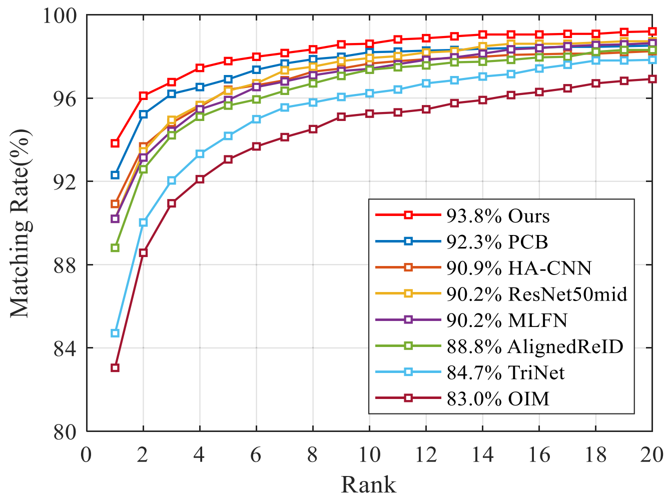


Fig. 14. The CMC curves and rank-1 accuracy on Market1501.

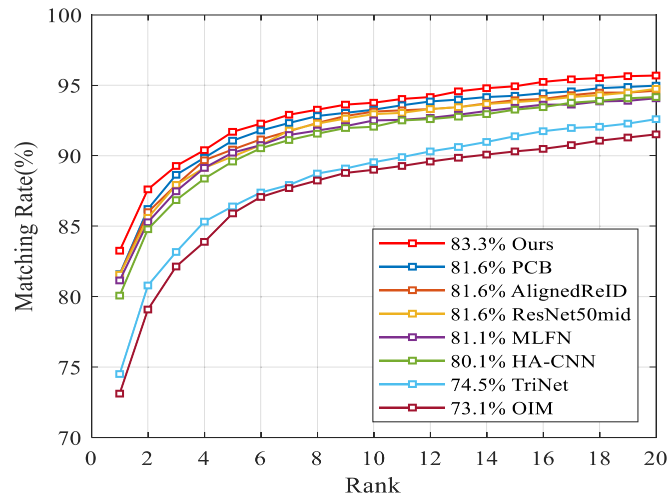


Fig. 15. The CMC curves and rank-1 accuracy on DukeMTMC-ReID.

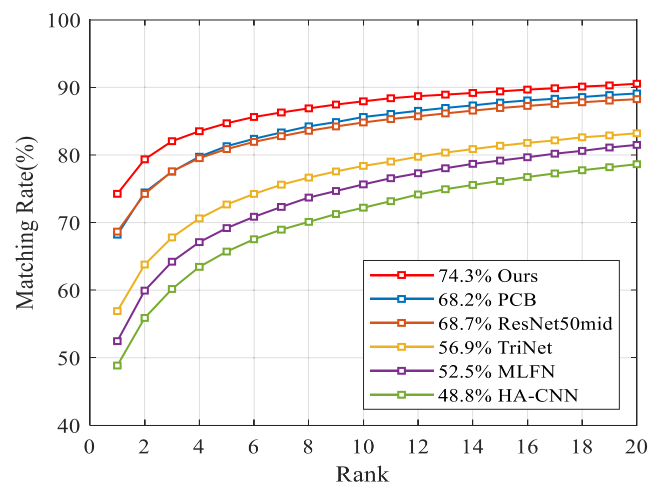


Fig. 16. The CMC curves and rank-1 accuracy on MSMT17.

*Results analysis on DukeMTMC-ReID dataset:* We also evaluated our method with other state-of-the-art methods on DukeMTMC-ReID dataset. Table II shows that our method again outperforms all compared state-of-the-arts methods with significant improvements on rank-1 and mAP, exceeding the PCB by 1.7% (83.3–81.6) in rank-1 and 1.8% (68.2–66.4) in mAP. Specifically, our method attains an 83.3% rank-1 accuracy and a 68.2% mAP.

*Results analysis on MSMT17 dataset:* We further evaluated our proposed method with other state-of-the-art methods on MSMT17, and the results are shown in Table III. The number of methods that report on this dataset is limited since it was only recently released. Our method is still superior to most state-of-the-art methods and attains the highest scores on rank-1 and mAP. Specifically, it achieves a 74.3% rank-1 accuracy and a 43.6% mAP, which outperforms the PCB by 6.1% (74.3–68.2) in rank-1 and 2.5% (43.6–41.1) in mAP.

As we can see, the experimental results on three large-scale benchmarks, including Market1501, DukeMTMC-ReID, and MSMT17, demonstrate that our method outperforms most existing state-of-the-art methods and sufficiently show the robustness and efficiency of our method for Re-ID.

*2) Further Ablation Analysis and Discussion:* We further evaluated the performance of each part of our center-triplet model on Market1501 and DukeMTMC-ReID: the fusion feature learning network (FFLN) and hard mining center-triplet loss (HCTL).

*Effect of the fusion feature learning network:* We conducted experiments with different pooling operations on the standard ResNet50 and evaluated them with rank-1, 5, 10 accuracies and mAP to illustrate the robustness of the FFLN, which learns fusion features by combining max pooling and average pooling. We also conducted additional comparative experiments to verify the effect of the last stride after the Conv5 layer and the dropout in the fusion layer. The results for two datasets are shown in Tables IV, V and Figs. 17–18. Avg stands for the ResNet50 with average pooling operation, Max stands for the ResNet50 with max pooling operation, Avg+Max stands for the FFLN (combining two pooling operations), +S1 stands for setting the last stride to 1, +S2 stands for setting the last stride to 2, and +Dropout stands for using dropout to avoid overfitting. All of them are optimized by softmax uniformly.

What we need to note the results is that learned features with a higher spatial resolution that improve performance do not apply to all Re-ID models. This applies to our model, although the effect is not very obvious. Applying dropout can also lead to a small improvement. The main contribution of FFLN is the fusion strategy of max pooling and average pooling. The FFLN with dropout and the last stride set to 1 can produce higher scores in rank-1 accuracy and mAP.

On Market1501, the model of ResNet50 with average pooling achieves an 82.0% rank-1 accuracy and a 63.6% mAP, which is similar to adopting a max pooling operation. By contrast, our FFLN (combine average pooling with a max pooling operation) achieves a 92.0% rank-1 accuracy and a 78.1% mAP, exceeding it by 10.0% and 14.5%. Compared with an efficient Re-ID model, such as PCB and HA-CNN, the FFLN still attains the highest scores in mAP, rank-5, and rank-10 accuracy and attains the second best rank-1.

TABLE IV
COMPARISON WITH MODELS ON MAEKER1501 DATASET. 1ST/2ND BEST IN RED/BLUE

| Model | mAP | Rank-1 | Rank-5 | Rank-10 |
|---|---|---|---|---|
| Avg+S2 | 63.6 | 82.0 | 92.8 | 95.2 |
| Max+S2 | 58.7 | 82.3 | 92.2 | 94.4 |
| Avg+S1 | 61.4 | 81.5 | 92.6 | 95.3 |
| Max+S1 | 55.3 | 80.0 | 90.9 | 94.1 |
| Avg+Max+S2 | 74.9 | 90.8 | 96.5 | 97.8 |
| Avg+Max+S2+ Dropout | 78.0 | 91.2 | 96.9 | 98.1 |
| Avg+Max+S1 | 75.1 | 91.4 | 97.0 | 98.0 |
| **Avg+Max+S1+ Dropout** | 78.1 | 92.0 | 97.3 | 98.2 |
| TriNet [10] | 69.0 | 84.7 | 94.2 | 96.2 |
| MLFN [42] | 74.5 | 90.2 | 95.9 | 97.4 |
| ResNet50-mid [47] | 76.1 | 90.2 | 96.4 | 97.9 |
| HA-CNN [14] | 75.6 | 90.9 | 96.4 | 97.8 |
| PCB [43] | 77.3 | 92.3 | 96.9 | 98.2 |

TABLE V
COMPARISON WITH MODELS ON DukeMTMC-ReID DATASET. 1ST/2ND BEST IN RED/BLUE

| Model | mAP | Rank-1 | Rank-5 | Rank-10 |
|---|---|---|---|---|
| Avg+S2 | 48.5 | 68.9 | 82.4 | 86.6 |
| Max+S2 | 47.6 | 69.6 | 82.1 | 86.4 |
| Avg+S1 | 46.9 | 66.6 | 80.2 | 85.7 |
| Max+S1 | 47.7 | 70.3 | 82.0 | 86.0 |
| Avg+Max+S2 | 64.2 | 81.7 | 90.4 | 93.2 |
| Avg+Max+S2+ Dropout | 64.4 | 82.2 | 90.8 | 93.2 |
| Avg+Max+S1 | 64.3 | 82.0 | 90.4 | 92.9 |
| **Avg+Max+S1+ Dropout** | 64.7 | 82.3 | 90.9 | 93.6 |
| TriNet [10] | 57.7 | 74.5 | 86.4 | 89.5 |
| HA-CNN [14] | 63.2 | 80.1 | 89.6 | 92.1 |
| MLFN [42] | 63.2 | 81.1 | 90.3 | 92.6 |
| ResNet50-mid [47] | 64.0 | 81.7 | 90.0 | 93.0 |
| PCB [43] | 66.4 | 81.6 | 91.1 | 93.3 |

On DukeMTMC-ReID, the rank-1 and mAP are further improved to 82.3% and 64.7% in the FFLN, outperforming the original ResNet50 with average pooling by 13.4% and 16.2%, respectively. Likewise, compared with an efficient Re-ID model, such as PCB and HA-CNN, the FFLN attains the highest scores in rank-1 accuracy and the second-best mAP.

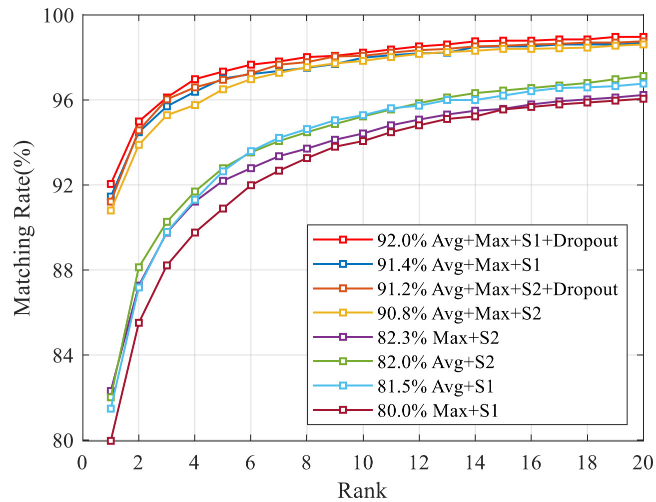


Fig. 17. Comparisons with different pooling operations on Market1501.

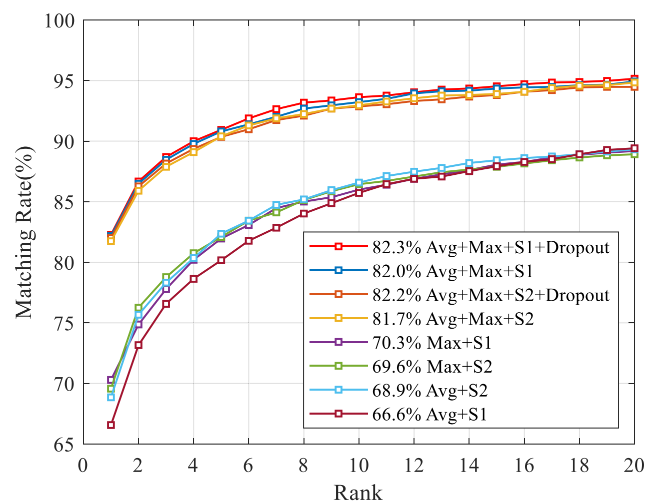


Fig. 18. Comparisons with different pooling operations on DukeMTMC-ReID.

In order to further illustrate the superiority of the FFLN in robust feature learning, we output the visual retrieval results, as shown in Fig. 19. The first row shows the results for the method using ResNet50 with an average pooling operation. According to the retrieval results, 3 false matches in the top 8 nearest images were all dark in contrast and brightness, which proves that average pooling takes low response features into consideration, thereby reducing the contrast in the feature map. Regarding max pooling, 2 false matches in the top 4 nearest images both show bright color characteristics and contrast, especially the first false match. It shows that max pooling is sensitive to high response features and ignores the low response values, discriminative features. Both of them have difficulties in learning robust feature representation. In contrast, the FFLN combines the advantages of max pooling and average pooling, which can learn high response values, bright features, and low response values,


Fig. 19. Visual retrieval results with different pooling operations. The green rectangle represents correct matches, and the red dash rectangle represents false matches. For the query sample, the first, second, and third rows show the results for the methods of ResNet50 with an average pooling operation, ResNet50 with a max pooling operation, and the FFLN, respectively.

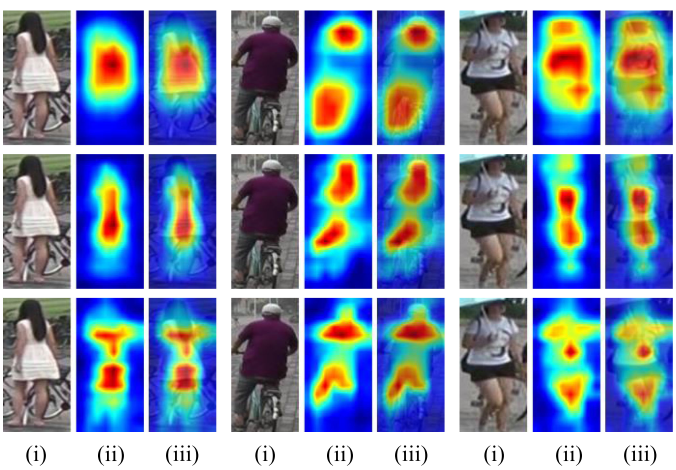


Fig. 20. Visualization of the Conv5 feature maps learned by different pooling operations. The first, second, and third rows show the results for the methods of ResNet50 with an average pooling operation, ResNet50 with a max pooling operation, and the FFLN, respectively. From left to right, (i) Original images, (ii) Activation map, and (iii) Overlapped image. In the heat map, the response increases from blue to red.

TABLE VI
SCORES OF DIFFERENT LOSS FUNCTIONS FOR RE-ID ON MARKET1501 DATASET. THE BEST SCORES ARE IN RED

| Method | mAP | Rank-1 | Rank-5 | Rank-10 |
|---|---|---|---|---|
| Classic Triplet | 54.8 | 75.9 | 89.6 | -- |
| Quadruplet | 61.1 | 80.0 | 91.8 | -- |
| Softmax | 63.6 | 82.0 | 92.8 | 95.2 |
| OIM | 62.5 | 83.0 | 93.1 | 95.2 |
| Softmax+Ring loss | 66.9 | 83.4 | 93.5 | 95.7 |
| Softmax+Center loss | 66.4 | 84.1 | 94.2 | 96.3 |
| Softmax+Range loss | 66.2 | 84.4 | 94.0 | 96.1 |
| Softmax+CWTL | 68.0 | 85.2 | 93.6 | 96.0 |
| Trihard | 69.0 | 84.7 | 94.2 | 96.2 |
| Cluster loss | 71.5 | 86.1 | 95.0 | -- |
| Softmax+TCL | 69.8 | 86.3 | 94.2 | 96.3 |
| **Softmax+HCTL（Our）** | 73.8 | 88.4 | 95.5 | 97.3 |

TABLE VII
SCORES OF DIFFERENT LOSS FUNCTIONS FOR RE-ID ON DukeMTMC-ReID DATASET. THE BEST SCORES ARE IN RED

| Method | mAP | Rank-1 | Rank-5 | Rank-10 |
|---|---|---|---|---|
| Softmax | 48.5 | 68.9 | 82.4 | 86.6 |
| Softmax+Center loss | 50.0 | 70.0 | 83.3 | 87.6 |
| Softmax+Ring loss | 51.3 | 70.7 | 83.5 | 87.0 |
| Softmax+CWTL | 52.0 | 72.2 | 84.2 | 88.0 |
| Softmax+TCL | 53.2 | 72.1 | 84.4 | 88.6 |
| Softmax+Range loss | 54.1 | 73.3 | 85.5 | 89.0 |
| OIM loss | 54.6 | 73.1 | 85.9 | 91.5 |
| Trihard loss | 57.7 | 74.5 | 86.4 | 89.5 |
| **Softmax+HCTL（Our）** | 55.8 | 75.2 | 87.0 | 90.4 |

discriminative features simultaneously, thereby enhancing the contrast in the feature map. It can also be seen from the matching results that the top 8 nearest images in the third row are all correctly matched with distinctive features. In addition, we visualize the final output feature maps learned by different pooling operations, as shown in Fig. 20. We notice that the feature maps from the ResNet50 with average pooling and ResNet50 with max pooling both produce poor representations. By contrast, the FFLN can force the network to focus more on the person region.

Compared with adopting a single deterministic pooling operation, the experimental results show the superiority of the FFLN in learning robust feature representation, which obtains deep fusion features by adjusting the weights of features learned by the two pooling operations.

*Effect of the hard mining center-triplet loss:* We also conduct experiments with different loss functions on ResNet50 to illustrate the robustness of the proposed HCTL. The results on the two datasets are shown in Tables VI, VII and Figs. 21–22. Classic Triplet stands for the classic triplet loss [19], Quadruplet stands for quadruplet loss [22], OIM stands for Online Instance Matching Loss [44], Cluster loss stands for cluster loss [45], Trihard stands for the trihard loss [10], and Softmax stands for softmax loss with LSR. We also combine ring loss [50], center loss [20], range loss [51], class-wise triplet loss (CWTL) [26], triplet-center loss (TCL) [27], and our hard mining center-triplet loss (HCTL) with Softmax.

On Market1501, as clearly seen in Table VI, the HCTL gets a 73.8% mAP and an 88.4% rank-1 accuracy, which outperforms

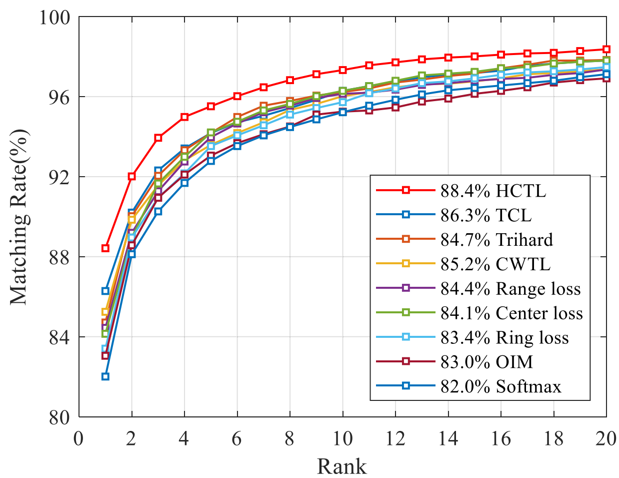


Fig. 21. Comparisons with different loss functions on Market1501.

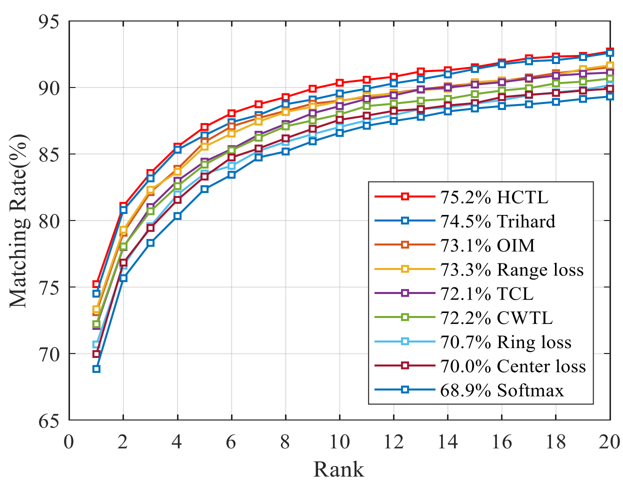


Fig. 22. Comparisons with different loss functions on DukeMTMC-ReID.

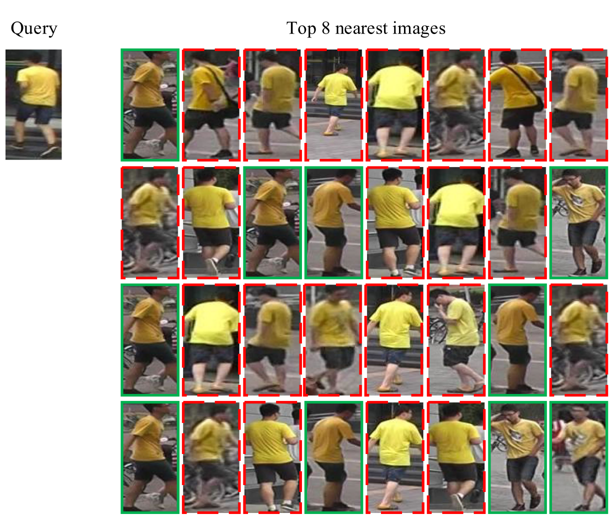


Fig. 23. Visual retrieval results on Market1501. The green rectangle represents correct matches, and the red dash rectangle represents false matches. For each sample, the first, second, third, and fourth rows show the results for the methods of ResNet50+Softmax, ResNet50+Softmax+HCTL, FFLN+Softmax and FFLN+Softmax+HCTL, respectively.


Fig. 24. Visual retrieval results on DukeMTMC-ReID. The green rectangle represents correct matches, and the red dash rectangle represents false matches. For each samples, the first, second, third, and fourth rows show the results for the methods of ResNet50+Softmax, ResNet50+Softmax+HCTL, FFLN+Softmax and FFLN++Softmax+HCTL, respectively.

all compared losses, exceeding the second-best TCL by 2.1% (88.4-86.3) in rank-1 and 4% (73.8-69.8) in mAP. Compared with softmax loss, adding HCTL can increase the accuracy by 6.4% on rank-1 and by 10.2% on mAP.

On DukeMTMC-ReID, the HCTL also attains the highest rank-1 accuracy and the second-best mAP. Although performance does not improve much compared with trihard loss, fewer hard triplets are mined for training with our HCTL. The significantly reduces the computing and mining requirements of hard training samples. Compared with softmax loss, adding HCTL can increase the rank-1 accuracy and mAP by 6.3% and 7.3%.

Compared with similar loss functions overall, our loss is more efficient in training networks and optimizing the intra/inter-class distance and reducing the computing and mining requirements of hard training samples simultaneously.

In summary, it can be seen that the FFLN contributes more than HCTL, but they are both important to the overall model. Once the FFLN trained by softmax loss has converged, the HCTL can further encourage the clustering of features of samples and achieve superior performance.

A comparison of visual retrieval results on the two datasets between our method and the ResNet50 with softmax (baseline) is shown in Figs. 23–24. Both FFLN and HCTL have made great contributions to the center-triplet model. Finally, our method significantly improved the Re-ID in comparison to the baseline, which also outperforms most state-of-the-art methods.

## V. Conclusion

In this paper, we proposed a novel center-triplet model for person re-identification. Firstly, we designed a fusion feature learning network. It was shown to learn high response values, bright features, and low response values, discriminative features simultaneously and obtains more discriminative fusion features by adaptively learning the weights of the features using max pooling and average pooling. In addition, we designed a hard mining center-triplet loss, a novel improved triplet loss, which builds the most challenging triplets for computing loss. It is shown to effectively optimize the intra/inter-class distance and reduce the computing and mining requirements of training hard samples simultaneously, thereby enhancing feature representation learning. Finally, the results show the robustness and efficiency of the proposed method. The model achieves a 93.8% rank-1 accuracy on Market1501, an 83.3% rank-1 accuracy on DukeMTMC-ReID, and a 74.3% rank-1 accuracy on MSMT17, outperforming most state-of-the-art methods for person re-identification. In the future, we would like to verify the robustness of our method on more datasets.

## Acknowledgment

The authors would like to thank the anonymous reviewers for their critical and constructive comments and suggestions.

## References

[1] W. Li, R. Zhao, T. Xiao, and X. Wang, "DeepReID: Deep filter pairing neural network for person re-identification," in *Proc. IEEE Conf. Comput. Vision Pattern Recognit.*, 2014, pp. 152–159.

[2] S. Wu *et al.*, "An enhanced deep feature representation for person re-identification," in *Proc. IEEE Winter Conf. Appl. Comput. Vision*, 2016, pp. 1–8.

[3] L. Wu, C. Shen, and A. van den Hengel, "Personnet: Person re-identification with deep convolutional neural networks," 2016. [Online]. Available: https://arxiv.org/abs/1601.07255

[4] H. Zhao *et al.*, "Spindle Net: Person re-identification with human body region guided feature decomposition and fusion," in *Proc. IEEE Conf. Comput. Vision Pattern Recognit.*, 2017, pp. 1077–1085.

[5] D. Li, X. Chen, Z. Zhang, and K. Huang, "Learning deep context-aware features over body and latent parts for person re-identification," in *Proc. IEEE Conf. Comput. Vision Pattern Recognit.*, 2017, pp. 384–393.

[6] Z. Zheng, L. Zheng, and Y. Yang, "Pedestrian alignment network for large-scale person re-identification," *IEEE Trans. Circuits Syst. Video Technol.*, vol. 29, no. 10, pp. 3037–3045, Oct. 2019.

[7] K. Simonyan and A. Zisserman, "Very deep convolutional networks for large-scale image recognition," in *Proc. Int. Conf. Learn. Represent.*, 2014, pp. 1–14.

[8] C. Szegedy *et al.*, "Going deeper with convolutions," in *Proc. IEEE Conf. Comput. Vision Pattern Recognit.*, 2015, pp. 1–9.

[9] K. He, X. Zhang, S. Ren, and J. Sun, "Deep residual learning for image recognition," in *Proc. IEEE Conf. Comput. Vision Pattern Recognit.*, 2016, pp. 770–778.

[10] A. Hermans, L. Beyer, and B. Leibe, "In defense of the triplet loss for person re-identification," 2017. [Online]. Available: https://arxiv.org/abs/1703.07737

[11] X. Zhang *et al.*, "AlignedReID: Surpassing human-level performance in person re-identification," 2017. [Online]. Available: https://arxiv.org/abs/1711.08184

[12] Y. Lin *et al.*, "Improving person re-identification by attribute and identity learning," *Pattern Recognit.*, vol. 95, pp. 151–161, 2019.

[13] M. S. Sarfraz, A. Schumann, A. Eberle, and R. Stiefelhagen, "A pose-sensitive embedding for person re-identification with expanded cross neighborhood re-ranking," in *Proc. IEEE Conf. Comput. Vision Pattern Recognit.*, 2018, pp. 420–429.

[14] W. Li, X. Zhu, and S. Gong, "Harmonious attention network for person re-identification," in *Proc. IEEE Conf. Comput. Vision Pattern Recognit.*, 2018, pp. 2285–2294.

[15] L. Wei, S. Zhang, H. Yao, W. Gao, and Q. Tian, "GLAD: Global–local-alignment descriptor for scalable person re-identification," *IEEE Trans. Multimedia*, vol. 21, no. 4, pp. 986–999, Apr. 2018.

[16] Y. L. Boureau, J. Ponce, and Y. LeCun, "A theoretical analysis of feature pooling in visual recognition," in *Proc. 27th Int. Conf. Mach. Learn.*, 2010, pp. 111–118.

[17] D. Yu *et al.*, "Mixed pooling for convolutional neural networks," *Int. Conf. Rough Sets Knowl. Technol.*, Cham, Germany: Springer, 2014, pp. 364–375.

[18] G. Ding *et al.*, "Feature affinity based pseudo labeling for semi-supervised person re-identification," *IEEE Trans. Multimedia*, vol. 21, no. 11, pp. 2891–2902, Nov. 2019.

[19] S. Ding *et al.*, "Deep feature learning with relative distance comparison for person re-identification," *Pattern Recognit.*, vol. 48, no. 10, pp. 2993–3003, 2015.

[20] Y. Wen *et al.*, "A discriminative feature learning approach for deep face recognition," in *Proc. Eur. Conf. Comput. Vision*, 2016, pp. 499–515.

[21] D. Cheng, Y. Gong, S. Zhou, J. Wang, and N. Zheng, "Person re-identification by multi-channel parts-based CNN with improved triplet loss function," in *Proc. IEEE Conf. Comput. Vision Pattern Recognit.*, 2016, pp. 1335–1344.

[22] W. Chen, X. Chen, J. Zhang, and K. Huang, "Beyond triplet loss: A deep quadruplet network for person re-identification," in *Proc. IEEE Conf. Comput. Vision Pattern Recognit.*, 2017, pp. 403–412.

[23] Q. Xiao, H. Luo, and C. Zhang, "Margin sample mining loss: A deep learning based method for person re-identification," 2017. [Online]. Available: https://arxiv.org/abs/1710.00478

[24] R. Yu *et al.*, "Hard-aware point-to-set deep metric for person re-identification," in *Proc. Eur. Conf. Comput. Vision*, 2018, pp. 188–204.

[25] M. F. T Ali and S. Chaudhuri, "Maximum margin metric learning over discriminative nullspace for person re-identification," in *Proc. Eur. Conf. Comput. Vision*, 2018, pp. 122–138.

[26] Z. Ming, J. Chazalon, M. M. Luqman, M. Visani, and J. Burie, "Simple triplet loss based on intra/inter-class metric learning for face verification," in *Proc. IEEE Int. Conf. Comput. Vision Workshops*, 2017, pp. 1656–1664.

[27] X. He, Y. Zhou, Z. Zhou, S. Bai, and X. Bai, "Triplet-center loss for multi-view 3D object retrieval," in *Proc. IEEE Conf. Comput. Vision Pattern Recognit.*, 2018, pp. 1945–1954.

[28] C. Patruno, R. Marani, G. Cicirelli, E. Stella, and T. D'Orazio, "People re-identification using skeleton standard posture and color descriptors from RGB-D data," *Pattern Recognit.*, vol. 89, pp. 77–90, 2019.

[29] Y. Guo, G. Zhao, and M. PietikäInen, "Discriminative features for texture description," *Pattern Recognit.*, vol. 45, no. 10, pp. 3834–3843, 2012.

[30] C. Zhao *et al.*, "Multiple metric learning based on bar-shape descriptor for person re-identification," *Pattern Recognit.*, vol. 71, pp. 218–234, 2017.

[31] C. Zhao *et al.*, "Maximal granularity structure and generalized multi-view discriminant analysis for person re-identification," *Pattern Recognit.*, vol. 79, pp. 79–96, 2018.

[32] C. Zhao *et al.*, "Similarity learning with joint transfer constraints for person re-identification," *Pattern Recognit.*, vol. 97, 2020, Art. no. 107014.

[33] N. Srivastava *et al.*, "Dropout: A simple way to prevent neural networks from overfitting," *J. Mach. Learn. Res.*, vol. 15, no. 1, pp. 1929–1958, 2014.

[34] C. Szegedy, V. Vanhoucke, S. Ioffe, J. Shlens, and Z. Wojna, "Rethinking the inception architecture for computer vision," in *Proc. IEEE Conf. Comput. Vision Pattern Recognit.*, 2016, pp. 2818–2826.

[35] H. Luo *et al.*, "Bags of tricks and a strong baseline for deep person re-identification," 2019, *arXiv:1903.07071*.

[36] L. Zheng *et al.*, "Scalable person re-identification: A benchmark," in *Proc. IEEE Int. Conf. Comput. Vision*, 2015, pp. 1116–1124.

[37] Z. Zheng, L. Zheng, and Y. Yang, "Unlabeled samples generated by GAN improve the person re-identification baseline in vitro," in *Proc. IEEE Int. Conf. Comput. Vision*, 2017, pp. 3754–3762.

[38] E. Ristani *et al.*, "Performance measures and a data set for multi-target, multi-camera tracking," in *Proc. Eur. Conf. Comput. Vision*, 2016, pp. 17–35.

[39] S. J. Reddi, S. Kale, and S. Kumar, "On the convergence of Adam and beyond," in *Proc. Int. Conf. Learn. Represent.*, 2018, pp. 1–23.

[40] S. Liao, Y. Hu, X. Zhu, and S. Z. Li, "Person re-identification by local maximal occurrence representation and metric learning," in *Proc. IEEE Conf. Comput. Vision Pattern Recognit.*, 2015, pp. 2197–2206.

[41] Y. Sun, L. Zheng, W. Deng, and S. Wang, "SVDNet for pedestrian retrieval," in *Proc. IEEE Int. Conf. Comput. Vision*, 2017, pp. 3800–3808.

[42] X. Chang, T. M. Hospedales, and T. Xiang, "Multi-level factorisation net for person re-identification," in *Proc. IEEE Conf. Comput. Vision Pattern Recognit.*, 2018, pp. 2109–2118.

[43] Y. Sun *et al.*, "Beyond part models: Person retrieval with refined part pooling (and a strong convolutional baseline)," in *Proc. Eur. Conf. Comput. Vision*, 2018, pp. 480–496.

[44] T. Xiao, S. Li, B. Wang, L. Lin, and X. Wang, "Joint detection and identification feature learning for person search," in *Proc. IEEE Conf. Comput. Vision Pattern Recognit.*, 2017, pp. 3415–3424.

[45] D. Alex *et al.*, "Cluster loss for person re-identification," 2018. [Online]. Available: https://arxiv.org/abs/1812.10325

[46] Y. Chen, X. Zhu, and S. Gong, "Person re-identification by deep learning multi-scale representations," in *Proc. IEEE Int. Conf. Comput. Vision*, 2017, pp. 2590–2600.

[47] Q. Yu *et al.*, "The devil is in the middle: Exploiting mid-level representations for cross-domain instance matching," 2017. [Online]. Available: https://arxiv.org/abs/1711.08106

[48] L. Qi *et al.*, "MaskReID: A mask based deep ranking neural network for person re-identification," 2018. [Online]. Available: https://arxiv.org/abs/1804.03864

[49] X. Bai *et al.*, "Deep-person: Learning discriminative deep features for person re-identification," 2020, vol. 98, Art. no. 107036.

[50] Y. Zheng, D. K. Pal, and M. Savvides, "Ring loss: Convex feature normalization for face recognition," in *Proc. IEEE Conf. Comput. Vision Pattern Recognit.*, 2018, pp. 5089–5097.

[51] X. Zhang, Z. Fang, Y. Wen, Z. Li, and Y. Qiao, "Range loss for deep face recognition with long-tailed training data," in *Proc. IEEE Int. Conf. Comput. Vision*, 2017, pp. 5409–5418.

[52] L. Wei, S. Zhang, W. Gao, and Q. Tian, "Person transfer GAN to bridge domain gap for person re-identification," in *Proc. IEEE Conf. Comput. Vision Pattern Recognit.*, 2018, pp. 79–88.

[53] K. Zhou and T. Xiang, "Torchreid: A library for deep learning person re-identification in pytorch," 2019. [Online]. Available: https://arxiv.org/abs/1910.10093

[54] C. Zhao *et al.*, "Multilevel triplet deep learning model for person re-identification," *Pattern Recognit. Lett.*, vol. 117, pp. 161–168, 2019.


**Cairong Zhao** received the B.Sc. degree from Jilin University, Changchun, China, in 2003, the M.Sc. degree from the Changchun Institute of Optics, Fine Mechanics and Physics, Chinese Academy of Sciences, Beijing, China, in 2006, and the Ph.D. degree from the Nanjing University of Science and Technology, Nanjing, China, in 2011. He is currently an Associate Professor with Tongji University, Shanghai, China. He is the author of more than 30 scientific papers in pattern recognition, computer vision, and related areas. His research interests include computer vision, pattern recognition, and visual surveillance.

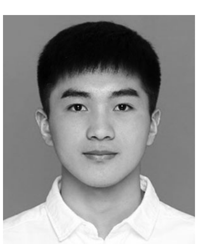

**Xinbi Lv** is currently working toward the master's degree with the College of Electronics and Information Engineering, Tongji University, Shanghai, China. His research interests include computer vision, deep learning, and person search, in particular, focusing on person re-identification and person search for visual surveillance.

**Zhang Zhang** received the B.Sc. degree in computer science and technology from the Hebei University of Technology, Tianjin, China, in 2002, and the Ph.D. degree in pattern recognition and intelligent systems from the National Laboratory of Pattern Recognition, Institute of Automation, Chinese Academy of Sciences, Beijing, China, in 2008. He is currently an Associate Professor with the National Laboratory of Pattern Recognition, Institute of Automation, Chinese Academy of Sciences. He has authored a number of papers at top venues, including the IEEE TRANSACTIONS ON PATTERN ANALYSIS AND MACHINE INTELLIGENCE, CVPR, and ECCV. His research interests include human attribute recognition, person re-identification, and activity recognition.

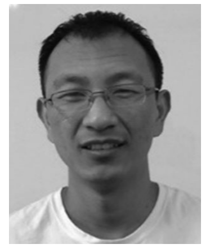

**Wangmeng Zuo** (Senior Member, IEEE) received the Ph.D. degree in computer application technology from the Harbin Institute of Technology, Harbin, China, in 2007. From 2004 to 2006, he was a Research Assistant with the Department of Computing, The Hong Kong Polytechnic University. From 2009 to 2010, he was a Visiting Professor with Microsoft Research Asia. He is currently a Professor with the School of Computer Science and Technology, Harbin Institute of Technology. He has authored more than 90 papers in top-tier academic journals and conferences. His current research interests include image enhancement and restoration, image generation and editing, visual tracking, object detection, and image classification. He was a Tutorial Organizer in ECCV 2016, he was an Associate Editor for the *IET Biometrics,* and the Guest Editor for *Neurocomputing, Pattern Recognition*, IEEE TRANSACTIONS ON CIRCUITS AND SYSTEMS FOR VIDEO TECHNOLOGY, and the IEEE TRANSACTIONS ON NEURAL NETWORKS AND LEARNING SYSTEMS.

**Jun Wu** (Senior Member, IEEE) received the B.Sc. degree in information engineering and the M.Sc. degree in communication and electronic systems from Xidian University, Xi'an, China, in 1993 and 1996, respectively, and the Ph.D. degree in signal and information processing from the Beijing University of Posts and Telecommunications, Beijing, China, in 1999. He is a Professor with the Computer Science and Technology Department, Tongji University, Shanghai, China. He joined Tongji University as a Professor in 2010. He was a Principal Scientist with Huawei and Broadcom before he joined Tongji. His research interests include wireless communication, information theory, machine learning, and signal processing.

**Duoqian Miao** was born in 1964. He is a Professor and a Ph.D. Tutor with the College of Electronics and Information Engineering, Tongji University, Shanghai, China and he serves as the Vice President of the International Rough Set Society, an Executive Manager of the Chinese Association for Artificial Intelligence, Chair of the CAAI Granular Computing Knowledge Discovery Technical Committee, a distinguished member of Chinese Computer Federation, the Vice President of the Shanghai Computer Federation, and the Vice President of the Shanghai Association for Artificial Intelligence. He serves as Associate Editor for the *International Journal of Approximate Reasoning* and an Editor of the *Journal of Computer Research and Development* (in Chinese). He has authored more than 200 papers in the IEEE TRANSACTIONS ON CYBERNETICS, IEEE TRANSACTIONS ON INFORMATION FORENSICS AND SECURITY, IEEE TRANSACTIONS ON KNOWLEDGE AND DATA MINING, IEEE TRANSACTIONS ON FUZZY SYSTEMS, *Pattern Recognition*, *Information Sciences*, *Knowledge-Based Systems*, *Chinese Journal of Computers*, *Journal of Software* (in Chinese), *Journal of Computer Research and Development* (in Chinese), *Automatica Sinica* (in Chinese), and *ACTA Electronica Sinica* (in Chinese). His interests include machine learning, data mining, big data analysis, granular computing, artificial intelligence, and text image processing. He won the Second Prize at Wuwenjun AI Science and Technology (2018).